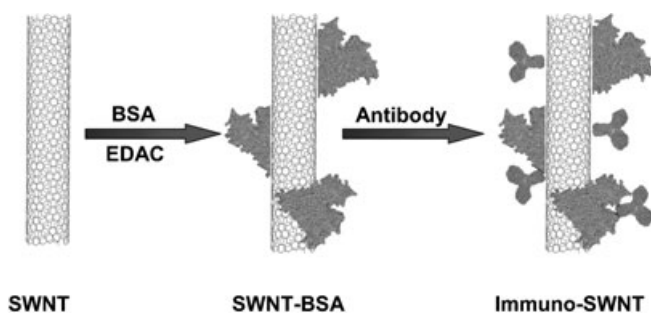


## Immuno-Carbon Nanotubes and Recognition of Pathogens

Tara Elkin, Xiuping Jiang, Shelby Taylor, Yi Lin, Lingrong Gu, Hua Yang, Jessica Brown, Susan Collins, and Ya-Ping Sun\*<sup>[a]</sup>

Carbon nanotubes have been widely investigated for their unique combination of properties including their one-dimensional hollow structure, high-strength with flexibility, large surface area, and chemical stability.<sup>[1,2]</sup> There has also been growing interest in their potential biological applications, especially in biosensors<sup>[2]</sup> and vaccine- and drug-delivery systems.<sup>[3,4]</sup> Both single- and multiple-walled carbon nanotubes (SWNT and MWNT, respectively) can be modified and conjugated with bioactive molecules and biological species including carbohydrates,<sup>[5,6]</sup> amino acids and peptides,<sup>[7–9]</sup> nucleic acids and analogues,<sup>[10–12]</sup> and proteins.<sup>[13–16]</sup> We have previously demonstrated that SWNTs are naturally protein affinitive in water and that covalent modification of the nanotubes with proteins gives stable conjugation and excellent aqueous solubility of the conjugates.<sup>[15]</sup> Here we report the preparation of immuno-carbon nanotubes by conjugating pathogen-specific antibodies to the SWNTs that are functionalized with bovine serum albumin (BSA) protein (Scheme 1) and, for the first time, the recognition of target pathogen cells by the immuno-carbon nanotubes via antibody–antigen interactions in physiological environment.



Scheme 1.

The SWNT–BSA conjugate was prepared by a carbodiimide-activated amidation reaction of the nanotube-bound carboxylic acids with pendant amino moieties on BSA.<sup>[14a]</sup> The conjugate sample was readily soluble in water (nanotube equivalent solubility  $> 5 \text{ mg mL}^{-1}$ ), forming a dark-colored but homoge-

neous solution. The solution was used to cast a solid-state thin film for optical absorption measurements. The spectrum thus obtained exhibits near-IR absorption bands at  $\sim 1900$  and  $\sim 1010 \text{ nm}$  that are characteristic of the first ( $S_{11}$ ) and second ( $S_{22}$ ) van Hove singularity transitions of semiconducting SWNTs, respectively.<sup>[17]</sup> Atomic force microscopy (AFM) imaging of the sample on a mica surface shows that the BSA-functionalized SWNTs are well dispersed and that each nanotube is intimately associated with multiple BSA species (Figure 1). These results agree well with those already available in the literature,<sup>[14]</sup> thus confirming the formation of an SWNT–BSA conjugate.

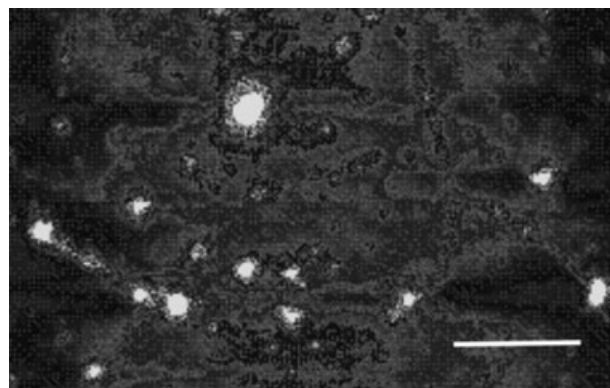


Figure 1. An AFM image of the SWNT–BSA sample on a mica surface (scale bar =  $1 \mu\text{m}$ ).

The nanotube-bound protein species can be selectively removed in the thermal gravimetric analysis (TGA) to allow an estimate of the nanotube content.<sup>[18]</sup> According to the TGA result,  $25 \pm 5\%$  ( $w/w$ ) of a typical SWNT–BSA conjugate sample is nanotube. The conjugate sample was also analyzed in a modified Lowry assay to determine the total protein content.<sup>[14]</sup> The result of  $\sim 70\%$  ( $w/w$ ) total protein in the sample (with the rest being primarily SWNTs) is consistent with the nanotube content estimate based on TGA.

The SWNT–BSA conjugate was coated with the antibody goat anti-*Escherichia coli* O157 ( $\text{Ab}_1$ ) by direct adsorption. In a typical procedure, a solution of  $\text{Ab}_1$  ( $10 \mu\text{g mL}^{-1}$ ,  $90 \mu\text{L}$ ) in phosphate-buffered saline (PBS;  $0.1 \text{ M}$ ,  $\text{pH} \sim 7.4$ ) was added to the SWNT–BSA solution ( $20 \text{ mg mL}^{-1}$ ,  $100 \mu\text{L}$ ,  $0.1 \text{ M}$  PBS).<sup>[19]</sup> The mixture was subjected to slow rotation (DynaL Biotech Sample Mixer Model 947.01) at  $40 \text{ rpm}$  for  $20\text{--}24 \text{ h}$  at room temperature, and then separated in a centrifuge at  $14000g$  (Eppendorf Centrifuge 5417R) to remove free  $\text{Ab}_1$  (in the discarded clear supernatant). The black pellet was resuspended in PBS buffer ( $100 \mu\text{L}$ ), and another round of the centrifuging/suspending process followed. The final sample was again suspended in PBS buffer ( $100 \mu\text{L}$ ) to yield a homogeneous dispersion of the SWNT–BSA– $\text{Ab}_1$  conjugate (or “immuno-SWNT”).

A solution of freshly cultured *E. coli* O157:H7 cells ( $100 \mu\text{L}$ ,  $0.85\%$  NaCl,  $\sim 10^9 \text{ CFU mL}^{-1}$ ) was added to the immuno-SWNT solution ( $100 \mu\text{L}$ ,  $0.1 \text{ M}$  PBS). The mixture was subjected to slow rotation at  $40 \text{ rpm}$  for  $1 \text{ h}$  at room temperature, and then separated in a centrifuge at  $14000g$ . The pellet was repeatedly

[a] T. Elkin, Prof. X. Jiang, S. Taylor, Dr. Y. Lin, L. Gu, H. Yang, J. Brown, S. Collins, Prof. Y.-P. Sun  
Department of Chemistry, Howard L. Hunter Chemistry Laboratory and Department of Food Science and Human Nutrition  
Poole Agriculture Center, Clemson University  
Clemson, SC 29634 (USA)  
Fax: (+1) 864-656-5007  
E-mail: syaping@clemson.edu

Supporting information for this article is available on the WWW under <http://www.chembiochem.org> or from the author.

washed with PBS buffer to remove unbound immuno-SWNT species, and the final suspension in PBS was passed through a membrane filter (0.2  $\mu\text{m}$ ). The filter with the immuno-SWNT-bound *E. coli* cells was used as the specimen (after the application of a thin conductive coating) for scanning electron microscopy (SEM) analysis. The SEM images thus obtained provide visual evidence for the conclusion that there are indeed strong interactions between the immuno-SWNT and *E. coli* cells. In fact, the *E. coli* cells are covered by SWNTs, as shown in Figure 2.

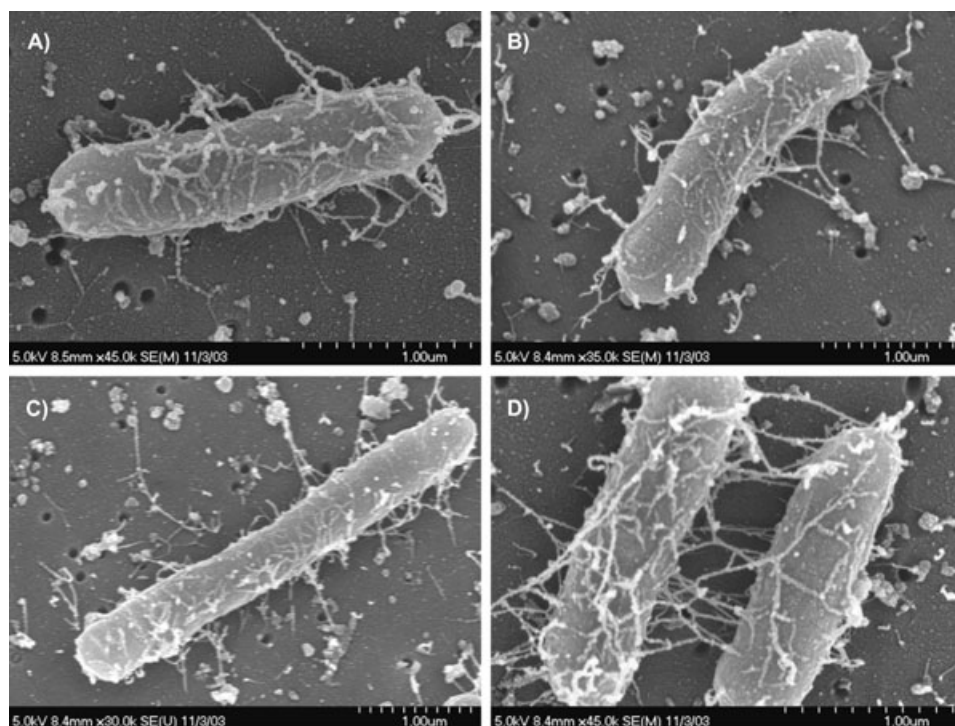


**Figure 2.** SEM images of *E. coli* cells bound with immuno-SWNT species. There was the possibility occasionally to find two cells bound together by the nanotubes (D). This became even rarer when the bacteria concentration was lower.

The interactions of the immuno-SWNT with *E. coli* cells are specific. In a control experiment, the SWNT-BSA conjugate rather than the immuno-SWNT was used with the *E. coli* cells in the same experimental procedure. However, the SEM results suggest no meaningful binding of the nanotube conjugates with the *E. coli* cells (Figure 3). The cells in these images are in sharp contrast to those from the *E. coli*-immuno-SWNT sample (Figure 2). Evidently, the immunofunctionality induced by the coating of SWNT-BSA with  $\text{Ab}_1$  is critical to the binding with the *E. coli* cells. The results also suggest that SWNTs conjugated with immunofunctionalities are indeed bioactive and capable of specific antibody-antigen interactions with pathogenic cells.

The specific antibody-antigen interactions were verified in terms of the use of a secondary antibody, goat anti-rabbit IgG (H+L) ( $\text{Ab}_2$ ). The secondary antibody  $\text{Ab}_2$  is such that it binds only to the primary antibody ( $\text{Ab}_1$ ) but not to the *E. coli*.<sup>[20]</sup> To enable confocal microscopy imaging, *E. coli* cells labeled with a green fluorescent protein (GFP) marker<sup>[21]</sup> and secondary anti-

body  $\text{Ab}_2$  labeled with rhodamine (red fluorescence) were used. In the experiment, a solution of  $\text{Ab}_2$  ( $5 \mu\text{g mL}^{-1}$ ,  $15 \mu\text{L}$ ,  $0.1 \text{ M}$  PBS) was added to a mixture of the immuno-SWNT and *E. coli* cells ( $15 \mu\text{L}$ ,  $0.01 \text{ M}$  PBS), and the resulting sample was incubated at  $37^\circ\text{C}$  for 30 min. After centrifuging at  $10000g$ , the sample was washed repeatedly with PBS ( $0.01 \text{ M}$ ) to remove unbound  $\text{Ab}_2$ , and then resuspended in PBS. A small drop of the suspension was placed on a glass slide and sealed with a glass cover slip for confocal microscopy analysis.

In the confocal microscopy imaging, the green fluorescence spots (Figure 4A) identify the *E. coli* cells (GFP-labeled), and the red fluorescence spots (Figure 4B) identify the  $\text{Ab}_2$  species (rhodamine-labeled). Figure 4C shows a combination of the two images, in which the yellow fluorescence spots are due to the superposition of the green and red signals. Since  $\text{Ab}_2$  only binds to  $\text{Ab}_1$  but not to *E. coli* and there was no free  $\text{Ab}_1$  as a result of the thorough washing, the confocal microscopy results suggest strongly that the antibody-antigen interactions with the *E. coli* cells are specific to  $\text{Ab}_1$  in the immuno-SWNT.

The immuno-SWNT-*E. coli* interactions are through the nanotube-bound  $\text{Ab}_1$  species and the cell surface antigen sites. In immuno-SWNT, the initial nanotube conjugation with BSA introduces the necessary aqueous solubility, making it easier to further modify the nanotubes in a physiologically compatible environment.<sup>[19]</sup> However, the ad-

sorption mode of the antibodies onto the SWNT-BSA is probably complex, including the issue of whether the nanotube-bound BSA species repel or facilitate the conjugation with the antibodies. Several possibilities for the adsorption mode will be evaluated in further investigations.<sup>[22]</sup>

It is known that the conformational structures of the antibody proteins might play a critical role in some antibody-antigen interactions.<sup>[23]</sup> For the antibody  $\text{Ab}_1$ , possible changes in its conformation upon being attached to the SWNT-BSA conjugate remain to be explored and understood. It does appear, however, that whatever the effect might be, it does not fundamentally change the immunological function of the SWNT-bound antibody species. The observation of clearly strong interactions between the immuno-SWNT and the target *E. coli* cell suggests that the conjugated antibodies are capable of specific recognition toward their antigen counterparts. Similarly, Dai and co-workers reported that some antigens that were immobilized onto SWNT devices by covalent linkages to surfac-

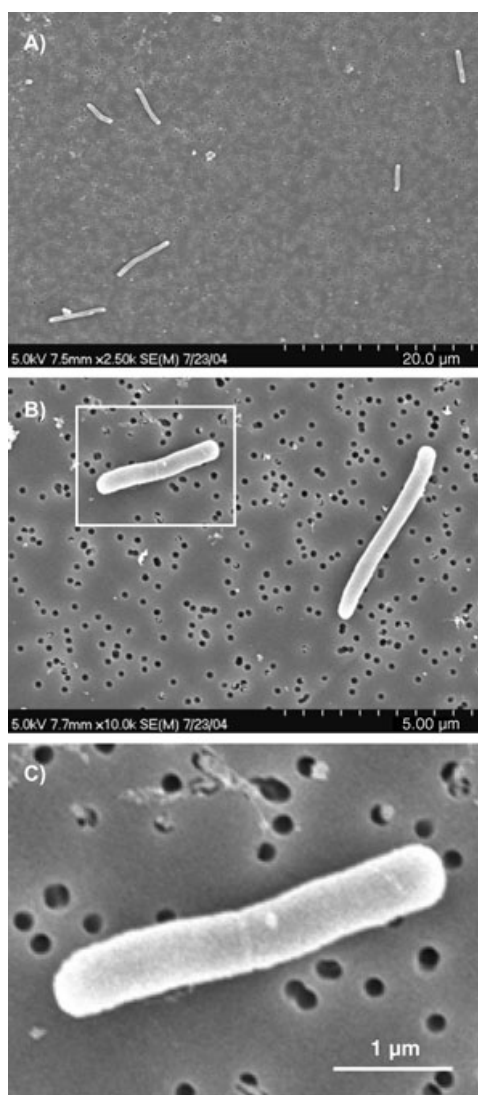


**Figure 3.** SEM images of the sample from the control experiment in which SWNT-BSA without  $Ab_1$  was used.

tant molecules still retained activity toward their antibody counterparts.<sup>[13a]</sup>

In summary, we have shown that the antibody goat anti-*E. coli* O157 can be conjugated to the SWNT-BSA conjugate to form the immuno-SWNT under physiologically compatible conditions. The immuno-SWNT is capable of recognizing pathogenic *E. coli* O157:H7 cells through specific antibody-antigen interactions. Carbon nanotubes are species of unique properties, such as large aspect ratio and high surface area. These nanomaterial properties are being explored for biosensors and related bioapplications. The work reported here might prove valuable to the potential development of rapid and ultrasensitive pathogen-detection techniques based on the use of carbon nanotubes.

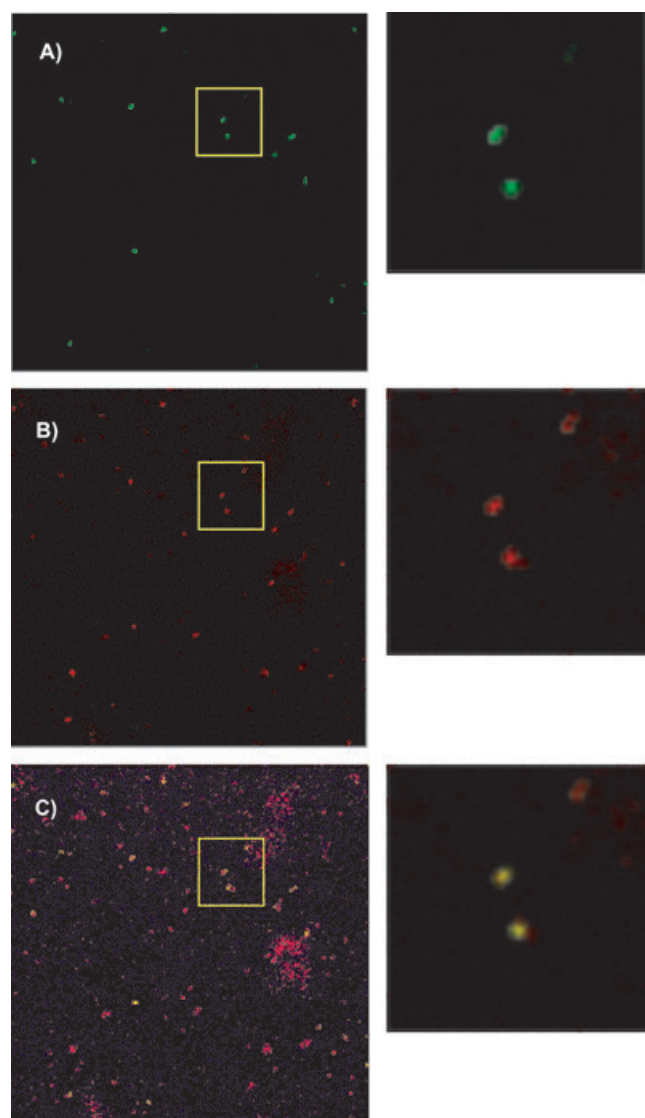


**Figure 4.** Confocal microscope images of A) green fluorescent protein-labeled *E. coli*, B) red fluorescent rhodamine-labeled  $Ab_2$  bound to immuno-SWNT, and C) yellow spots from a combination of (A) and (B).

## Acknowledgements

We thank Prof. M. P. Doyle for providing the *E. coli* strain, Prof. A. M. Rao for supplying the nanotube sample, and S. Fernando and B. Zhou for experimental assistance. Financial support from NSF is gratefully acknowledged. J.B. and S.C. were participants of the Summer Undergraduate Research Program sponsored jointly by NSF and Clemson University.

**Keywords:** biological activity · immunoassays · nanostructures · nanotubes

[1] P. M. Ajayan, *Chem. Rev.* **1999**, *99*, 1787–1799.

[2] Y. Lin, S. Taylor, H. Li, K. A. S. Fernando, L. Qu, W. Wang, L. Gu, B. Zhou, Y.-P. Sun, *J. Mater. Chem.* **2004**, *14*, 527–541.

[3] A. Bianco, M. Prato, *Adv. Mater.* **2003**, *15*, 1765–1768.

- [4] N. W. S. Kam, T. C. Jessop, P. A. Wender, H. Dai, *J. Am. Chem. Soc.* **2004**, *126*, 6850–6851.
- [5] F. Pompeo, D. E. Resasco, *Nano Lett.* **2002**, *2*, 369–373.
- [6] a) A. Star, D. W. Steuerman, J. R. Heath, J. F. Stoddart, *Angew. Chem.* **2002**, *114*, 2618–2622; *Angew. Chem. Int. Ed.* **2002**, *41*, 2508–2512; b) O.-K. Kim, J. Je, J. W. Baldwin, S. Kooi, P. E. Pehrsson, L. J. Buckley, *J. Am. Chem. Soc.* **2003**, *125*, 4426–4427.
- [7] V. Georgakilas, N. Tagmatarchis, D. Pantarotto, A. Bianco, J.-P. Briand, M. Prato, *Chem. Commun.* **2002**, 3050–3051.
- [8] a) D. Pantarotto, C. D. Partidos, R. Graff, J. Hoebeke, J.-P. Briand, M. Prato, A. Bianco, *J. Am. Chem. Soc.* **2003**, *125*, 6160–6164; b) D. Pantarotto, C. D. Partidos, J. Hoebeke, F. Brown, E. Kramer, J.-P. Briand, S. Muller, M. Prato, A. Bianco, *Chem. Biol.* **2003**, *10*, 961–966.
- [9] G. R. Dieckmann, A. B. Dalton, P. A. Johnson, J. Razal, J. Chen, G. M. Giordano, E. Munoz, I. H. Musselman, R. H. Baughman, R. K. Draper, *J. Am. Chem. Soc.* **2003**, *125*, 1770–1777.
- [10] a) C. Dwyer, M. Guthold, M. Falvo, S. Washburn, R. Superfine, D. Erie, *Nanotechnology* **2002**, *13*, 601–604; b) S. E. Baker, W. Cai, T. L. Lasseter, K. P. Weidkamp, R. J. Hamers, *Nano Lett.* **2002**, *2*, 1413–1417; c) M. Hazani, R. Naaman, F. Hennrich, M. M. Kappes, *Nano Lett.* **2003**, *3*, 153–155.
- [11] K. A. Williams, P. T. M. Veenhuizen, B. G. de la Torre, R. Eritja, C. Dekker, *Nature* **2002**, *420*, 761.
- [12] a) M. Zheng, A. Jagota, E. D. Semke, B. A. Diner, R. S. McLean, S. R. Lustig, R. E. Richardson, N. G. Tassi, *Nat. Mater.* **2003**, *2*, 338–342; b) M. Zheng, A. Jagota, M. S. Strano, A. P. Santos, P. Barone, S. G. Chou, B. A. Diner, M. S. Dresselhaus, R. S. McLean, C. B. Onoa, G. S. Samsonidze, E. D. Semke, M. Usrey, D. J. Walls, *Science* **2003**, *302*, 1545–1548.
- [13] a) R. J. Chen, S. Bangsaruntip, K. A. Drouvalakis, N. W. S. Kim, M. Shim, Y. Li, W. Kim, P. J. Utz, H. Dai, *Proc. Natl. Acad. Sci. USA* **2003**, *100*, 4984–4989; b) M. Shim, N. W. S. Kam, R. J. Chen, Y. Li, H. Dai, *Nano Lett.* **2002**, *2*, 285–288; c) R. J. Chen, H. C. Choi, S. Bangsaruntip, E. Yenilmez, X. Tang, Q. Wang, Y.-L. Chang, H. Dai, *J. Am. Chem. Soc.* **2004**, *126*, 1563–1568.
- [14] a) W. Huang, S. Taylor, K. Fu, Y. Lin, D. Zhang, T. W. Hanks, A. M. Rao, Y.-P. Sun, *Nano Lett.* **2002**, *2*, 311–314; b) K. Fu, W. Huang, Y. Lin, D. Zhang, T. W. Hanks, A. M. Rao, Y.-P. Sun, *J. Nanosci. Nanotechnol.* **2002**, *2*, 457–461.
- [15] Y. Lin, L. F. Allard, Y.-P. Sun, *J. Phys. Chem. B* **2004**, *108*, 3760–3764.
- [16] B. R. Azamian, J. J. Davis, K. S. Coleman, C. B. Bagshaw, M. L. H. Green, *J. Am. Chem. Soc.* **2002**, *124*, 12664–12665.
- [17] M. A. Hamon, M. E. Itkis, S. Niyogi, T. Alvaraez, C. Kuper, M. Menon, R. C. Haddon, *J. Am. Chem. Soc.* **2001**, *123*, 11292–11293.
- [18] Y.-P. Sun, K. Fu, Y. Lin, W. Huang, *Acc. Chem. Res.* **2002**, *35*, 1096–1104.
- [19] Sodium azide (0.02%) was used as a bacteriostatic agent in the stock solution of SWNT–BSA conjugate. It was removed by washing with PBS (centrifuging/redispersing) before the conjugate sample was used.
- [20] D. Wild, *The Immunoassay Handbook*, 2nd ed., Nature Publishing Group, New York, **2001**.
- [21] X. Jiang, J. Morgan, M. P. Doyle, *Appl. Environ. Microbiol.* **2002**, *68*, 2605–2609.
- [22] It is unclear whether antibodies are attached to the BSA or simply adsorb to free sites of the SWNTs uncovered by BSA.
- [23] J. Foote, *Science* **2003**, *299*, 1327–1328.

Received: September 22, 2004

Published online on March 1, 2005